VERIFICATION OF SPECTRAL REDUCTION FACTORS FOR SEISMIC ASSESSMENT OF BRIDGES

C. Casarotti[1], R. Monteiro[2] and R. Pinho[3]

SUMMARY

Within a nonlinear static analysis procedure perspective for the assessment of structures, one of the key issues is the employment of a demand spectrum that takes also into account, through an adequate reduction of its spectral ordinates, the hysteretic energy dissipation capacity of the structure being assessed. There are certainly a relatively large number of past parametric studies dedicated to the validation of different approaches to translate such structural energy dissipation capacity into spectral reduction factors, however such studies have focused mainly, if not exclusively, on single-degree-of-freedom (SDOF) systems. It seems, therefore, that verification on full structural systems, such as complete bridges, is conspicuously needed in order to verify the adequacy of using existing SDOF-derived relationships in the assessment of multiple-degree-of-freedom (MDOF) systems. In this work, eleven different spectral reduction proposals, involving diverse combinations of previously proposed equivalent damping and spectral reduction equations, are evaluated, for various intensity levels, using a preliminarily validated nonlinear static procedure. A wide set of bridges, covering regular and irregular configurations as well as distinct support conditions, is used. The accuracy of the results is checked by direct comparison with Time-History Analyses performed with ten real ground motion records. Overall conclusions are then presented with the purpose of providing practitioners and researchers with indications on the most adequate spectral reduction schemes to be employed in nonlinear static analysis of bridges.

INTRODUCTION

For what seismic assessment of structures is concerned, the use of simplified procedures, such as pushover-based ones, may be considered as a useful alternative to the more rigorous nonlinear time-history analyses, if and when all relevant variables and effects are suitably taken into account. Those variables include, amongst others, the hysteretic damping associated to the energy dissipation capacity that a structure inherently presents during an earthquake. One of the main concerns, when applying any Nonlinear Static Procedure (NSP), is thus the definition of a demand spectrum that features ordinates appropriately scaled-down to take due account of the aforementioned capacity of structures for dissipating seismic energy through hysteresis.

Reduction of spectral ordinates may be carried out through the use of either over-damped elastic or constant-ductility inelastic spectra. The former make use of equations that estimate, as a function of ductility, values of the so-called equivalent viscous damping which is then used as input into another set of expressions that provide the spectral scaling factor. In alternative, the use of constant-ductility inelastic spectra, although perhaps less commonly, has also been proposed as a means to estimate seismic demand within the scope of nonlinear static assessment of structures [e.g. 1, 2].

There are a relatively large number of past parametric studies dedicated to the derivation and/or validation of different approaches to estimate spectral reduction factor values [e.g. 3, 4], however such studies seem to have focused mainly, if not exclusively, on single-degree-of-freedom (SDOF) systems. It seems, therefore, that verification on full structural systems is conspicuously needed in order to verify the adequacy of using existing SDOF-derived relationships in the assessment of multiple-degree-of-freedom (MDOF) systems.

In the present work, the case of bridges is considered (building frames are being currently investigated through a separate endeavour), and eleven different approaches for taking into account, through spectral scaling, the energy dissipation capacity of such systems are considered. In order to do so, the Adaptive Capacity Spectrum Method (ACSM), recently proposed by Casarotti and Pinho [5] is employed as the reference nonlinear static procedure. The method starts by assuming an initial start-up target damping/ductility value, with which the scaled response spectrum is then computed, after which the intersection between the latter and the capacity curve is calculated, and the corresponding ductility/damping determined, carrying out a new iteration in case the latter differs from the initial assumption. The rationale behind such choice is the fact that it has been shown [6, 7] that ACSM provides bridge seismic performance predictions that are superior (or equivalent in worst cases) to those obtained from other NSPs commonly used in practice.

The accuracy of bridge behaviour predictions, in terms of displacements, shear forces or bending moments obtained at the performance point using each of the selected spectral reduction possibilities, is evaluated throughout direct comparison with results from Nonlinear Time-History Analyses, carried out for a sufficiently large number of ground motion records. The study is performed for a wide range of bridge configurations as well as different support conditions.

[1] *C. Casarotti, European Centre for Training and Research in Earthquake Engineering (EUCENTRE), Pavia, Italy*

[2] *R. Monteiro, University of Porto, Civil Engineering Department, Porto, Portugal*

[3] *R. Pinho, University of Pavia, Structural Mechanics Department, Pavia, Italy*

SPECTRAL REDUCTION FACTORS

As previously discussed, spectral Reduction Factors (RF) can be roughly divided in two groups: damping-based and ductility-based. Roughly, the first family consists of all those methods which, through the application of a reduction factor B based on the equivalent viscous damping (elastic viscous plus hysteretic), reduce by the same amount both displacement and acceleration spectral ordinates (see equation (1) and Figure 1 left). To the second category belong all those approaches which make use of a 5%-damping elastic response spectrum and then reduce the spectral acceleration ordinates by a factor defined as a function of ductility (equation (2) and Figure 1 right). The spectral reduction within ductility-based methods is not exactly vertical, given that displacements are modified as well, however, for the range of periods considered in this work, R ≈ μ. A few hybrid methodologies have also been proposed, as discussed subsequently.

$$S_{a,damp} = B \cdot S_{a,el-5\%}$$
$$S_{d,damp} = B \cdot S_{d,el-5\%} \quad (1)$$
$$S_{d,damp} = \frac{S_{a,damp}}{\omega^2}$$

$$S_{a,duct} = \frac{S_{a,el-5\%}}{R} \quad (2)$$
$$S_{d,duct} = \frac{\mu}{R} S_{a,el-5\%} = C \cdot S_{d,el-5\%}$$

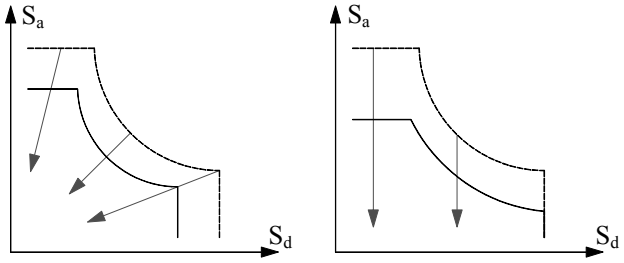

Figure 1: Spectral reduction methods: damping-based (left) and ductility-based (right).

Damping-based methods

With regard to damping-based spectrum scaling methods, a combination of different ways of calculating the (i) equivalent viscous damping ξ_{eq} and (ii) corresponding spectral reduction factor B are available. Some of the most commonly used ones are presented and reviewed in what follows.

Equivalent viscous damping models

In the following equations, ξ_0 stands for the so-called elastic viscous damping and μ for ductility (which was a variable of the work, given that it varied with the intensity level and the characteristics of the response of each bridge).

A) ATC40, based on the modified Rosenblueth and Herrera model (herein termed *ATC40*)

This proposal by Rosenblueth and Herrera [8], and subsequently adopted by ATC40 [9], was the first equivalent linear method to suggest the use of secant stiffness at maximum deformation as the basis for considering inelastic response. In such approach, if one considers a bilinear system with a post-yield stiffness ratio α, the viscous damping for the equivalent linear elastic system is given by equation (3), where κ is an empirical parameter that takes account the degree to which the hysteresis response cycle resembles a parallelogram or not; three possibilities are defined (A, B or C), depending on structural system configuration and duration of ground shaking.

$$\xi_{eq-ATC40} = \xi_0 + \kappa \frac{2}{\pi}\left[\frac{(1-\alpha)(\mu-1)}{\mu - \alpha\mu + \alpha\mu^2}\right] \quad (3)$$

B) Kowalsky, based on the Takeda hysteretic model with post-yield hardening (herein termed *TakKow*)

Kowalsky [10] derived an equation for equivalent viscous damping ratio that was based on the Takeda hysteretic model. For a thin response mode (empirical parameter b = 0) with unloading stiffness factor of 0.5 and a post-yield stiffness ratio α, the equivalent damping ratio is given by equation (4).

$$\xi_{eq-TakKow} = \xi_0 + \frac{1}{\pi}\left[1 - \frac{(1-\alpha)}{\sqrt{\mu}} - \alpha\sqrt{\mu}\right] \quad (4)$$

C) Gulkan and Sozen, based on the Takeda model without hardening (herein termed *TakGS*)

Gulkan and Sozen [11] used the Takeda hysteretic model and experimental shaking table results of small-scale reinforced concrete frames to develop empirical equation (5) to compute equivalent viscous damping ratio values.

$$\xi_{eq-TakGulSoz} = \xi_0 + 0.2\left[1 - \frac{1}{\sqrt{\mu}}\right] \quad (5)$$

D) Iwan (herein termed *Iwan*)

Iwan [12] derived empirically equations to estimate the equivalent viscous damping ratio, equation (6), using a hysteretic model derived from a combination of elastic and Coulomb slip elements together with results from time-history analyses using 12 earthquake ground motion records.

$$\xi_{eq-Iwan} = \xi_0 + 0.0587 \cdot (\mu - 1)^{0.371} \quad (6)$$

E) Dwairi *et al*. (herein termed *Dwairi* or *DwaKowNau*)

Dwairi *et al*. [13] recently developed new equivalent viscous damping relations for four structural systems, defined as a function of ductility and effective period of vibration. With the latter, the authors claim to having managed to significantly reduce the error in predicting inelastic displacements and minimize the scatter of results. Considering the structural system that best fits the case of continuous deck bridges, the equivalent viscous damping relation is that shown in equation (7), where C_{ST} is a parameter dependent on the effective period, ranging from a minimum of 0.3 to a maximum value of 0.65.

$$\xi_{eq-DwaKowNau} = \xi_0 + \frac{C_{ST}}{\pi}\left(\frac{\mu-1}{\mu}\right) \quad (7)$$

F) Priestley *et al*. (herein termed *Priestley*)

The approach proposed by Priestley *et al*. [14] can, in a somewhat simplified manner, be represented by equation (8). Actually, the equation should be applied to each individual pier, and then a weighted average based on shear forces and response displacements would be used to estimate the overall damping of SDOF system. Herein, for reasons of simplicity and congruency with the employed NSP, the simplification of applying equation (8) directly to the full system is carried out.

$$\xi_{eq-Priestley} = \xi_0 + 0.444\left(\frac{\mu - 1}{\mu\pi}\right) \quad (8)$$

Figure 2 plots the six previously listed approaches for equivalent viscous damping estimation. It is noted that ATC40 results are computed for a structural type B (the most appropriate for the structures considered), no post-yield hardening was considered for ATC40 and TakKow approaches, and Dwairi's estimates are plotted for two representative values of 0.4 and 0.5.

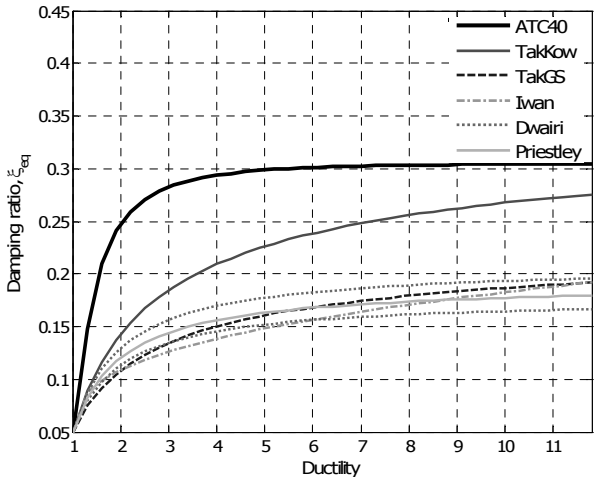

Figure 2: Considered damping models.

It is readily observed that whilst ATC40 and TakKow models distinguish themselves from the rest by providing significantly higher equivalent viscous damping estimates, the remaining four approaches (TakGS, Iwan, Dwairi, Priestley) yield results that are very close. With the latter in mind, and considering its relative contemporariness with the work of Gulkan and Sozen [11], the expression proposed by Iwan [12] will not be considered on the subsequent parametric study, also because, in opposite to the other relationships, it does not feature an upper bound limit. Such rationale could also have led to the exclusion of one the two proposals from Dwairi *et al.* [13] and Priestley *et al.* [14], however in this case both were kept in the parametric study given their diverse nature in terms of application.

Damping-based reduction factors

As previously discussed, the computation of ξ_{eq} is then followed by the calculation of the corresponding spectral reduction factor B. Different approaches may again be considered:

A) Newmark-Hall and ATC40 (herein termed *NH-ATC40*)

In the well known method proposed by Newmark and Hall [15], the damping reduction factors B_{NH} for median estimates of response (i.e. 50% probability of exceedance) are given by:

$$\begin{cases} B_{NH(acc)} = \dfrac{3.21 - 0.68\ln(100\xi_{eq})}{2.21}, & T_b \le T < T_c \\ B_{NH(vel)} = \dfrac{2.31 - 0.41\ln(100\xi_{eq})}{1.65}, & T_c \le T < T_d \\ B_{NH(disp)} = \dfrac{1.82 - 0.27\ln(100\xi_{eq})}{1.39}, & T \ge T_d \end{cases} \quad (9)$$

The data of Newmark and Hall were limited to viscous damping ratios of 20% and are obtained from a limited number of earthquakes prior to 1973. In addition they were derived from the displacement response spectrum or pseudo-acceleration response spectrum. It is noted that, for damping ratios higher than 5%, $B_{NH\,(acc)} < B_{NH\,(vel)} < B_{NH\,(disp)}$.

The method has been adapted by most of the American design codes and guidelines, such as the ATC-40 document [9], among others, where B_{ATC40} is defined by SR_A and SR_V, corresponding to constant acceleration and velocity regions, respectively:

$$\begin{cases} SR_A = \dfrac{3.21 - 0.68\ln(100\xi_{eq})}{2.21} \ge \overline{SR}_A & T < T_c \\ SR_V = \dfrac{2.31 - 0.41\ln(100\xi_{eq})}{1.65} \ge \overline{SR}_V & T \ge T_c \end{cases} \quad (10)$$

In both equations (9) and (10) a period $T_{c'}$ given by equation (11) should be applied in order to guarantee continuity conditions with respect to the corner period.

$$T_{c'} = \frac{B_{(vel)}}{B_{(acc)}} T_c \quad (11)$$

The constraints imposed by equation (10), referring to Table 1, depend on the aforementioned ATC40 structural typologies (A, B or C), and imply maximum admitted damping ratios of 37-40% for type A, 28-29% for type B and 19-20% for type C. Analogously, $SR_A < SR_V$.

Table 1. Maximum allowable SR_A, SR_V (ATC40) and SR_D (present study) values.

Structural Type	$\overline{SR}_A$	$\overline{SR}_V$	$\overline{SR}_D$
A	0.33	0.50	0.59
B	0.44	0.56	0.66
C	0.56	0.67	0.73

In the present study, an approach blending the proposals of Newmark and Hall [15] and ATC-40 [9] is taken into account. The original NH formulation is therefore complemented by considering the lower limits introduced by ATC40 for the velocity and acceleration zones, and introducing a factor SR_D (see Table 1) with a limitation similar to SR_A and SR_V, i.e., maximum admitted damping ratios of 40%, 29% and 20%, for types A, B and C respectively.

B) Eurocode 8 (herein termed *EC8*)

Eurocode 8 [16] recommends the use of the spectral reduction factors given in equation (12), with a minimum of 0.55.

$$B_{EC8} = \begin{cases} 1 - (1 - \eta)\dfrac{T}{T_b} & 0 \le T < T_b \\ \eta & T \ge T_b \end{cases} \quad (12)$$

$$\eta = \sqrt{\frac{10}{5 + 100\,\xi_{eq}}} \ge 0.55$$

C) Ramirez *et al.* (herein termed *Ramirez*)

Ramirez *et al*. [17] proposed a bilinear relationship – equation (13) – between the reduction factor B_{short} and equivalent damping ratio ξ_{eq}, valid up to damping ratios of 50%. Exceeding that value the relation becomes trilinear and dependent on B_{long} – equation (14). T_b and T_c are the first and third spectral characteristic/corner periods, whilst B_{short} and B_{long} can be found in Table 2.

$$B_{Ram} = \begin{cases} 1-(1-B_{short})\dfrac{T}{T_b} & 0 \le T < T_b \\ B_{short} & T \ge T_b \end{cases} \quad (13)$$

$$B_{Ram} = \begin{cases} 1-\left(1-B_{short}\right)\dfrac{T}{T_b} & 0 \le T < T_b \\ B_{long} - \left(B_{short} - B_{long}\right)\dfrac{\left(T-T_b\right)}{\left(T_c-T_b\right)} & T_b \le T < T_c \\ B_{long} & T \ge T_c \end{cases} \quad (14)$$

Table 2. Reduction factors for Ramirez et al. approach.

Equivalent damping, ξ (%)	B_{short}	B_{long}
5	1.00	B_{short}
10	0.83	B_{short}
20	0.67	B_{short}
30	0.59	B_{short}
40	0.53	B_{short}
50	0.45	B_{short}
60	0.43	0.38
70	0.43	0.34
80	0.42	0.30
90	0.41	0.27
100	0.40	0.25

D) Lin and Chang (herein termed *Lin-Chang*)

In a recent study, Lin and Chang [18] proposed a period-dependent reduction factor, equation (15), based on an extensive time-history analysis parametric study of linear elastic SDOF systems, using real USA records. Such RF has the advantage that, whilst still following the general trend of the others with respect to the structural period T, it is inherently continuous, hence not requiring the addition of any other type of continuity constraints or conditions.

$$B_{LinChang} = 1 - \frac{a\,T^{0.3}}{(T+1)^{0.65}} \quad (15)$$
$$a = 1.303 + 0.436\ln(\xi_{eq})$$

E) Priestley *et al.* (herein termed *Priestley*)

Recently, Priestley *et al*. [14] proposed the application of equation (16), which was included in earlier versions of Eurocode 8, but was then subsequently abandoned.

$$B_{Priestley} = \left(\frac{0.07}{0.02+\xi_0}\right)^{0.5} \quad (16)$$

Figure 3 presents results obtained with the above-listed spectral reduction equations for values of response period from three representative spectral regions; constant acceleration zone (T= $2T_b$), constant velocity zone (T= $2T_c$), constant displacement zone (T= $1.5T_d$). It is observed that those approaches that feature a lower bound limit (i.e. NH-ATC40, EC8 and Priestley) tend to yield the higher spectral reductions for low damping ratios (Priestley across the entire period range, EC8 in the displacement zone and NH-ATC40 in the acceleration zone). On the other hand, for higher values of damping (larger than 0.25-0.36) Ramirez and Lin-Chang equations provide the higher spectral reductions. The dispersion among the different proposals also increases with damping ratio.

Finally, it is perhaps also noteworthy to see that the NH-ATC40 formulae is highly sensitive to period values; if one considers a constant high value of damping (e.g. ξ_{eq} = 0.3), the spectral reduction factor may vary from 0.44 to 0.67, depending on the response period of the structure. To shed further insight into this latter issue (i.e. period dependency of spectral reductions), Figure 4 has also been produced. It is

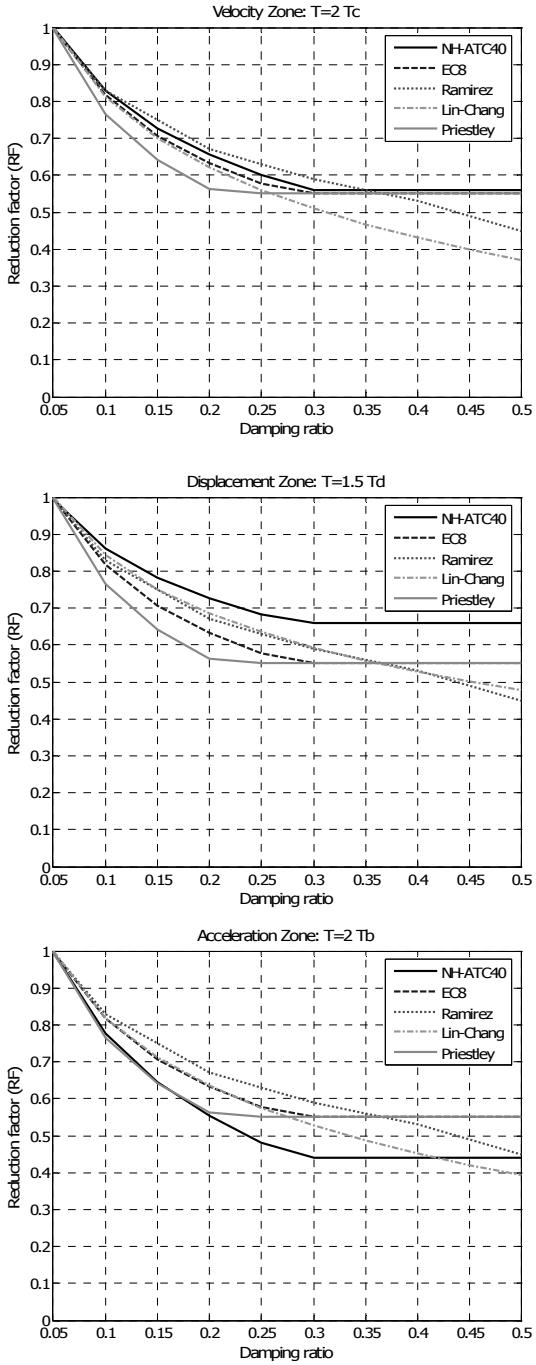

Figure 3: Reduction factor variation with damping in the three spectral regions.

observed that the dispersion among the several RF approaches, indicated in the plots as a percentage of the maximum RF, increases with the damping ratio. It is also noted that the NH-ATC40 variant generally yields the highest reduction factor, especially for periods higher than 3 or 4 seconds.

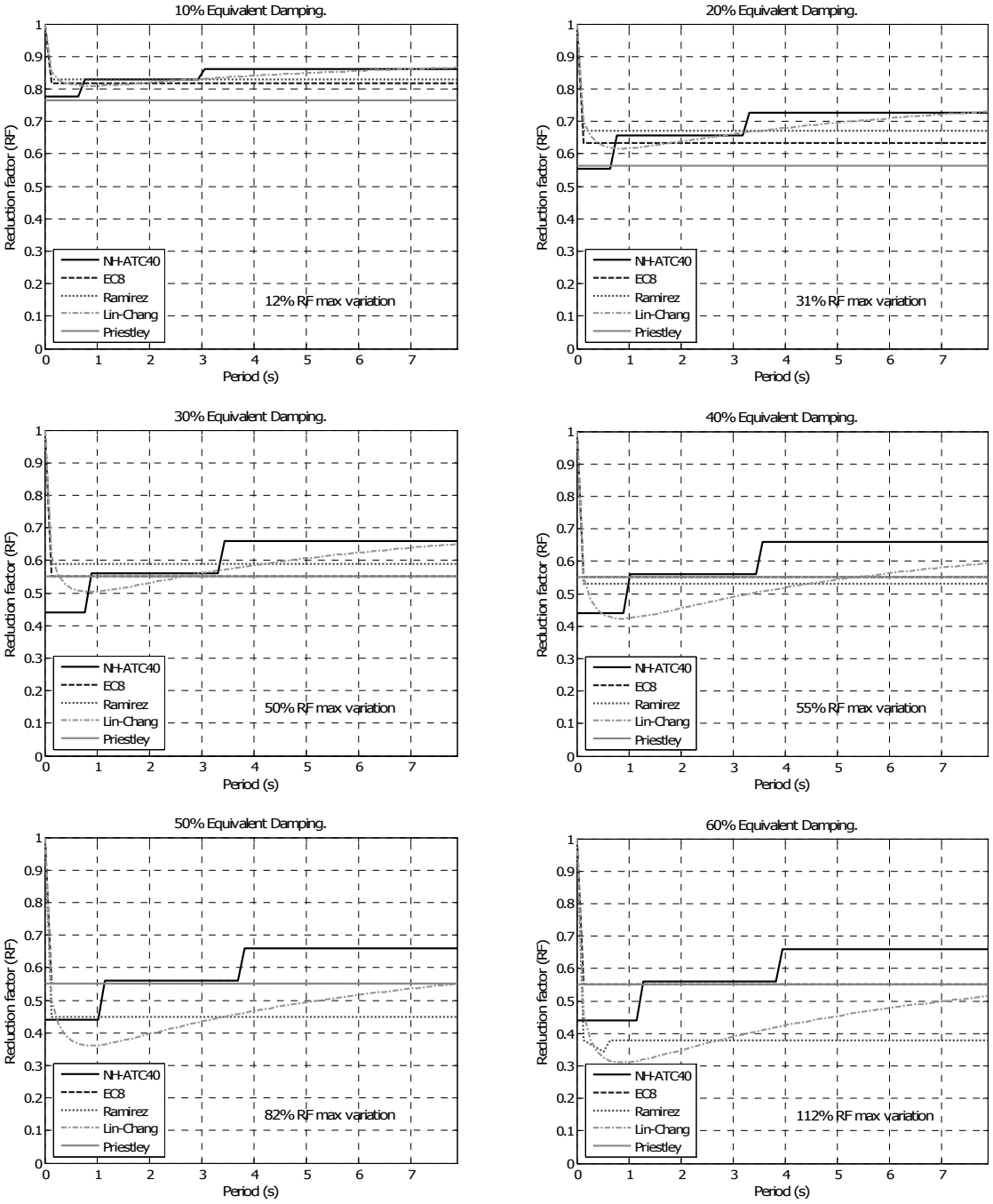

Figure 4: Reduction factor variation with period for different damping ratios.

In the parametric study described subsequently, three out of the above-listed five possible reduction factor approaches have been selected: (i) Lin-Chang (equation 15), (ii) Priestley (equation 16), (iii) a combination of EC8 and Ramirez (equation 17). This last hybrid approach, herein termed *EC8Ram*, aimed especially at creating a more simplified version of EC8 and Ramirez proposals that would nonetheless envelop the general period-dependent trend of RF; EC8 is employed for low periods where it yields lower RF estimates and Ramirez is considered for the high period range where it provides high RFs.

$$B_{EC8\_Ram} = \begin{cases} B_{EC8} & 0 \le T < T_{dd} = T_d \dfrac{B_{Ram}}{B_{EC8}} \\ B_{Ram} & T \ge T_{dd} \end{cases} \qquad (17)$$

The somewhat cumbersome trilinear NH-ATCH40 relationship was not considered further, whilst the equation by Priestley *et al.* [14] was employed only in tandem with the equivalent viscous damping equations proposed by the same authors (equation 8, above).

Ductility-based methods

As mentioned before, the reduction of the spectral ordinates may also be achieved by an alternative type of approach, whereby a reduction factor, directly dependent on ductility, is used. Amongst the different approaches present in literature, two have been considered in the current work:

A) Miranda (2000) for firm soils (herein termed *Mir2000*)

Miranda [4] observed that, for sites with average shear-wave velocities higher than 180 m/s in the upper 30 m of the soil profile (typically soil types A-B-C-D in ATC and FEMA

guideline documents), inelastic displacement ratios are not significantly affected by local site conditions, nor by changes in earthquake magnitude, nor by changes in epicentral distance (with the exception of very near-field sites that may be influenced by forward directivity effects). As a result, the following displacement modification factor expression was proposed:

$$C_{Mir} = \left[1 + \left(\frac{1}{\mu} - 1\right)\exp\left(-12T\,\mu^{-0.8}\right)\right]^{-1} \tag{18}$$

B) Vidic *et al.* (herein termed *VidFajFish*)

Vidic *et al* [19] suggested a relationship for a ductility-based reduction factor, with a corner period $T_{C'}$ dependent of the characteristic spectral period T_C, equation (19):

$$C_{VFF} = \begin{cases} \mu\left[1.35(\mu-1)^{0.95}\dfrac{T}{T_{c'}} + 1\right]^{-1} & T \le T_{c'} \\ \mu\left[1.35(\mu-1)^{0.95} + 1\right]^{-1} & T > T_{c'} \end{cases} \tag{19}$$

$$T_{c'} = 0.75\mu^{0.2}T_c \le T_c$$

In the parametric study that follows, a number of diverse spectrum scaling approaches will be employed, considering combinations of different equivalent viscous damping models and damping-based scaling factors, together with ductility-based scaling equations. With reference to the nomenclature introduced above, the eleven cases considered are hence: ATC40 - EC8Ram, ATC40 - LinChang, TakKow - EC8Ram, TakKow - LinChang, TakGS - EC8Ram, TakGS - LinChang, DwaKowNau - EC8Ram, DwaKowNau - LinChang, Priestley, Mir2000, VidFajFish.

PARAMETRIC STUDY – DESCRIPTION

The parametric study considered two bridge lengths (viaducts with four and eight 50 m spans), with regular, irregular and semi-regular layout of the piers' height and with two types of abutments; (i) continuous deck-abutment connections supported on piles, with a bilinear behaviour, and (ii) deck extremities supported on linear pot bearings. The total number of bridges is therefore fourteen, as implied by Figure 5, where the label numbers 1, 2 and 3 stand for pier heights of 7, 14 and 21 metres, respectively.

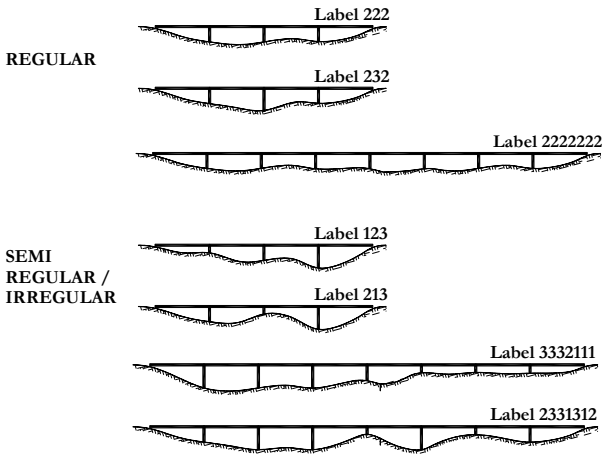

Figure 5: Bridge configurations.

The employed set of seismic excitation, referred to as LA, is defined by an ensemble of ten records selected from a suite of historical earthquakes scaled to match the 10% probability of exceedance in 50 years (475 years return period) uniform hazard spectrum for Los Angeles [21], which corresponds, in the current endeavour, to the intensity level 1.0. Additional intensity levels, linearly proportional by a factor of 0.5, 0.75, 1.5, 3.0 and 3.5, were also considered. The ground motions were obtained from California earthquakes with a magnitude range of 6-7.3 recorded on firm ground at distances of 13-30 km. The characteristics of the records are summarized in Table 3, where the significant duration is defined as the interval between the build up of 5% and 95% of the Total Arias Intensity [22]. Further details on the input motion can be found in [20].

The demand spectrum employed with the NSP was defined as the median response spectrum of the ten accelerograms, since individual accelerogram spectra contain singularities that are not only of limited significance from the statistical point of view, which stands at the base of RF relationships, but may constitute a source of convergence problems in the application of code-geared nonlinear static assessment methods, as shown by Miranda and Ruiz-García [3], for instance.

The seismic demand on the bridge models is evaluated by means of nonlinear time-history analyses (THA), with admitted equivalent viscous damping of 2%, assumed to constitute the most accurate tool to estimate the 'true' earthquake response of the structures, using the fibre-based finite elements program SeismoStruct [23], whose accuracy in predicting the seismic response of bridge structures has been demonstrated through comparisons with experimental results derived from pseudo-dynamic tests carried out on large-scale models [24]. The same software package was employed in the running of the displacement-based adaptive pushover analyses [25, 26] that are required by the employed nonlinear static procedure, ACSM. Within this sort of procedure, when computing elastic/inelastic response spectra, it is typical for 5% equivalent viscous damping to be included so as to account, amongst other things, for the pre-yield energy dissipation capacity of the structure (due to the fact that structural elements are not all cracked right from the start). This could sound inconsistent with the 2% assumed in THA. However, when carrying out fibre-modelling analysis, on the other hand, such pre-yield energy dissipation capacity is already implicitly accounted for in the element formulation, and thus needs not to be introduced by means of an equivalent viscous damping.

Table 3. Employed set of records.

Name	Earthquake	Duration	Significant Duration	PGA
LA 02	ElCentro, 1940	53.48 s	24.52 s	0.68 g
LA 04	Imperial Valley, 1979	39.38 s	7.09 s	0.49 g
LA 06	Imperial Valley, 1979	39.09 s	11.22 s	0.23 g
LA 08	Landers, 1992	79.98 s	22.24 s	0.43 g
LA 10	Landers, 1992	79.98 s	20.72 s	0.36 g
LA 12	Loma Prieta, 1989	39.98 s	6.40 s	0.97 g
LA 14	Northridge, 1994	59.98 s	5.52 s	0.66 g
LA 16	Northridge, 1994	14.95 s	7.04 s	0.58 g
LA 18	Northridge, 1994	59.98 s	5.30 s	0.82 g
LA 20	Palm Springs, 1986	59.98 s	6.78 s	0.99 g

Hence, the use of 2% equivalent viscous damping is typically employed. The two types of analysis or modelling approaches are thus equivalent, rendering possible the comparison of results of fibre analysis with 2% damping with results from 5% damped response spectra.

The results are presented in terms of different response parameters: the estimated displacement pattern (D) and flexural moments (M) of the bridge deck at the nodes above the piers, and the shear forces at the base of the piers (V) and abutments (ABT).

Then, in order to appraise the accuracy of the NSP results obtained with the different spectral reduction schemes, these are normalised with respect to the median of the corresponding response quantities obtained through the incremental THAs; this provides an immediate indication of the bias for each of the eleven spectral scaling procedures. Equation (20) shows, for a generalised parameter Δ at a given location i, how the results from the incremental dynamic analyses (IDA), run for each of the ten records considered, are first processed.

$$\hat{\Delta}_{i,IDA} = median_{j=1:10}\left[\Delta_{i,j-IDA}\right] \tag{20}$$

The aforementioned results' normalisation consists thus in computing, for each of the parameters and for each of the considered locations, the ratio between the result coming from ACSM application and the median result coming from THA, as illustrated in Figure 6 and numerically translated into equation (21); ideally the ratio should be one.

$$\overline{\Delta}_i = \frac{\Delta_{i,ACSM}}{\hat{\Delta}_{i,IDA}} \cdots \underset{ideally}{\rightarrow} 1 \tag{21}$$

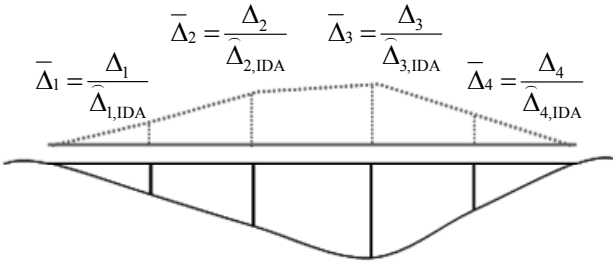

Figure 6: Normalised Transverse Deformed Pattern.

This normalisation renders also somewhat "comparable" all deck displacements, moments and shear forces, since all normalised quantities have the same unitary target value, thus allowing in turn the definition of a so-called bridge index [20]. The bridge index (BI) is computed as the median of normalised results for the considered parameter over the m deck locations; deck displacements (BI_D), deck moments (BI_M) or shear forces at the piers and abutments (BI_V and BI_{ABT}), as shown in equation (22). The standard deviation STD measures, on the other hand, the dispersion with respect to the median, for each of the eleven damping models – equation (23).

$$BI_{\Delta,\ ACSM\ version} = median_{i=1:m}\left[\overline{\Delta}_{i,ACSM\ version}\right] \tag{22}$$

$$STD_{\Delta} = \left[\frac{\sum_{i=1}^{m}\left(\overline{\Delta}_i - BI\right)^2}{m-1}\right] \tag{23}$$

PARAMETRIC STUDY – RESULTS

In the following, results are analysed to evaluate the validity of the different spectrum scaling approaches, starting from a somewhat global perspective, where the entire set of results (for all bridges and for all intensity levels) are first considered together, and then sub-structured in terms of seismic input and bridge model, in order to detect trends and dependencies, if possible.

Global results

This global results overview consists in the computation of the bridge index for each spectrum scaling approach over all the 14 bridges and 6 intensity levels. In other words, the median bridge index over all bridge configurations and intensity levels represents the median of the single BI of every considered bridge configuration, at every intensity level. Analogously, median standard deviation is also computed.

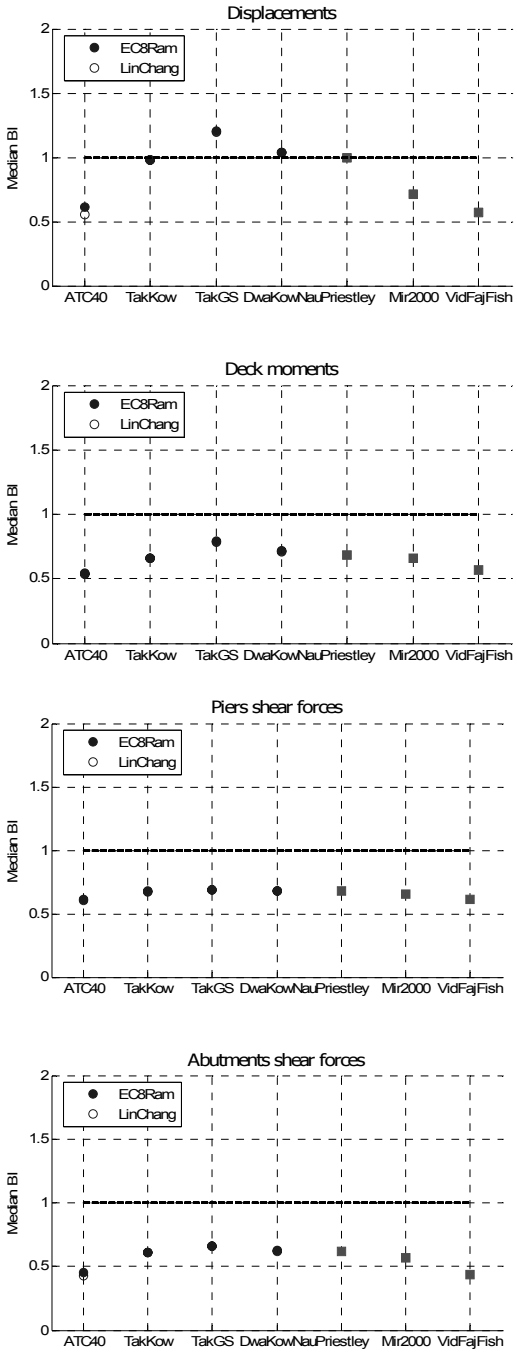

Figure 7: Global Bridge Index.

Figure 7 represents graphically the global median BI values and Table 4 features the corresponding STDs, both referring to each spectrum scaling modality.

Considering the results shown, the first conclusion is that it is the employed damping model, rather than the chosen damping-dependent spectral reduction equation, that conditions the results; there is essentially no difference between LinChang and EC8Ram results.

Table 4. Global Standard Deviation.

Method	D	V	M	ABT
ATC40 - EC8Ram	0.14	0.09	0.30	0.03
ATC40 - LinChang	0.13	0.09	0.30	0.03
TakKow - EC8Ram	0.23	0.09	0.38	0.04
TakKow - LinChang	0.23	0.09	0.38	0.04
TakGS - EC8Ram	0.34	0.09	0.42	0.03
TakGS - LinChang	0.32	0.09	0.41	0.03
DwaKowNau - EC8Ram	0.24	0.09	0.39	0.04
DwaKowNau - LinChang	0.23	0.09	0.40	0.04
Priestley	0.24	0.09	0.38	0.04
Mir2000	0.16	0.09	0.35	0.04
VidFajFish	0.14	0.09	0.31	0.03

Generally, it seems that the approaches TakKow, DwaKowNau and Priestley lead to the best global indexes, especially for what displacements are concerned, with a global median BI fairly close to one and median STD that is not excessive. On the other hand, the two ductility-based approaches (Mir2000 and VidFajFish) and the damping-based ATC40 method show the worst results when compared to nonlinear dynamic analyses. This trend seems to contradict opposite results, found in previous studies [1-2, 27-30], which state that inelastic spectra-based methods yield better results with respect to their elastic highly-damped counterparts. However, such findings come from the use of a different NSP from the used in the current framework, the Adaptive Capacity Spectrum Method (ACSM), which, within the elastic highly-damped methods, actually yields more consistent results in the assessment of the seismic response of bridges [6, 7] when compared to other NSPs, and this may explain the difference.

The underpredicting trend of ATC40 is probably due to the well known overprediction that such approach carries out within the equivalent damping estimation in structures which will not exactly exhibit elastoplastic behaviour.

Similar tendency is found when ductility based reduction factors are used. Mir2000 approach has been primarily developed for elastoplastic behaviour but has also been widely verified for other models such as Takeda or Clough, proving to work well for periods longer than 1.2 seconds, which is not the case of the considered bridge structures with maximum periods of about 0.8 seconds. One would therefore expect overprediction, as found by Miranda and Ruiz Garcia [3] for short periods. However, the low ductility levels achieved for the considered bridge structures have lead to barely unitary displacement modification factors. VidFajFish approach, on the other hand, is known to be highly dependent on period and ductility for the short period region, which may apply to the selected bridge structures; for this region, the R factor increases linearly with increasing period, remaining constant for the rest of the periods, which may cause some excessive reduction, and, hence, under prediction, given that periods tend to be low, as early stated, for this sort of structures.

The Gulkan and Sozen approach, based on the Takeda hysteretic model, is over predicting displacements. According to equation (5) and Figure 2, it is the one with lowest equivalent damping prediction, among all the approaches, for ductility levels not higher than approximately 3. Adding to this the fact that most cases of application correspond to ductility levels equally distributed between 1 and 3, one may explain the overprediction by the underestimation of damping-based energy dissipation.

The superiority found when using TakKow, DwaKowNau or Priestley approaches is firstly, in opposite to the others, due to the intermediate nature on estimating the equivalent viscous damping. Additionally, the latter two, which are the most recent, have been particularly developed and therefore, more suitable, to the structural behaviour where bridges fit in. DwaKowNau's equation, for instance, depends on the effective period which is another advantage, whereas Priestley's expression refers exactly to bridge piers.

Intensity level results

Herein, at each intensity level, the median Bridge Index and Standard Deviation over the 14 bridge configurations is computed for all possible spectrum scaling modalities. For reasons of succinctness, only displacements and piers shear forces results are presented in Figure 8, the former being then repeated in Table 5, to assist in the interpretation of the results.

Observing this new set of results, it turns out apparent that amongst the three approaches previously mentioned to be performing superiorly, the one proposed by Priestley *et al.* [14] seems to be slightly better, even if only marginally, very closely followed by those of Kowalsky [10] and Dwari *et al.* [13]. The latter approach seems then to introduce a not relevant dependency of the coefficient C_{ST} on the effective period. In addition, it is also noted that there is a general tendency for the displacements' predictions to improve with increasing intensity level, probably due to the fact that for low levels of nonlinearity, thus dissipation, current damping and RF relationships overestimate the reduction, whilst for the case of piers shear forces, the opposite is instead verified, since higher intensity levels are associated to a decrease in the accuracy of the NSP predictions. No noteworthy influence of the intensity level was found in deck moments and abutment forces results.

As expected (see Figure 2), ATC40 damping model seems to overestimate damping, leading to underestimated displacements at each intensity level.

As for the standard deviation, this did increase with growing intensity in the case of deck displacements (e.g. from 0.18 to 0.33 with the Priestley approach), but was instead constant for all other response parameters. Again, generally, the worst modalities predicting Bridge Index have lower, but not considerably different, dispersion levels, as can be confirmed by the displacement-only results given in Table 6.

Bridge configuration results

Herein, for each bridge configuration, the median Bridge Index and Standard Deviation across the 6 intensity levels is plotted considering each of the eleven possible modalities for energy dissipation (i.e. spectrum scaling) modelling. A bridge configuration detailed level of results enables the analysis of the influence of symmetry, regularity, length, abutments type, among other variables, on the global results previously presented and discussed.

Figures 9 and 10 show the median BI and STD across all intensity levels, for each bridge configuration. Again, for the sake of brevity, only displacement results are shown. As expected, the response predictions do appear to be very bridge-dependent, even if the observations/conclusions previously drawn still hold for the majority of configurations; e.g. the Priestley approach consistently leads to the closest-to-unity BIs. It was also observed, though it is not shown herein, that variations in the accuracy of deck moments and shear

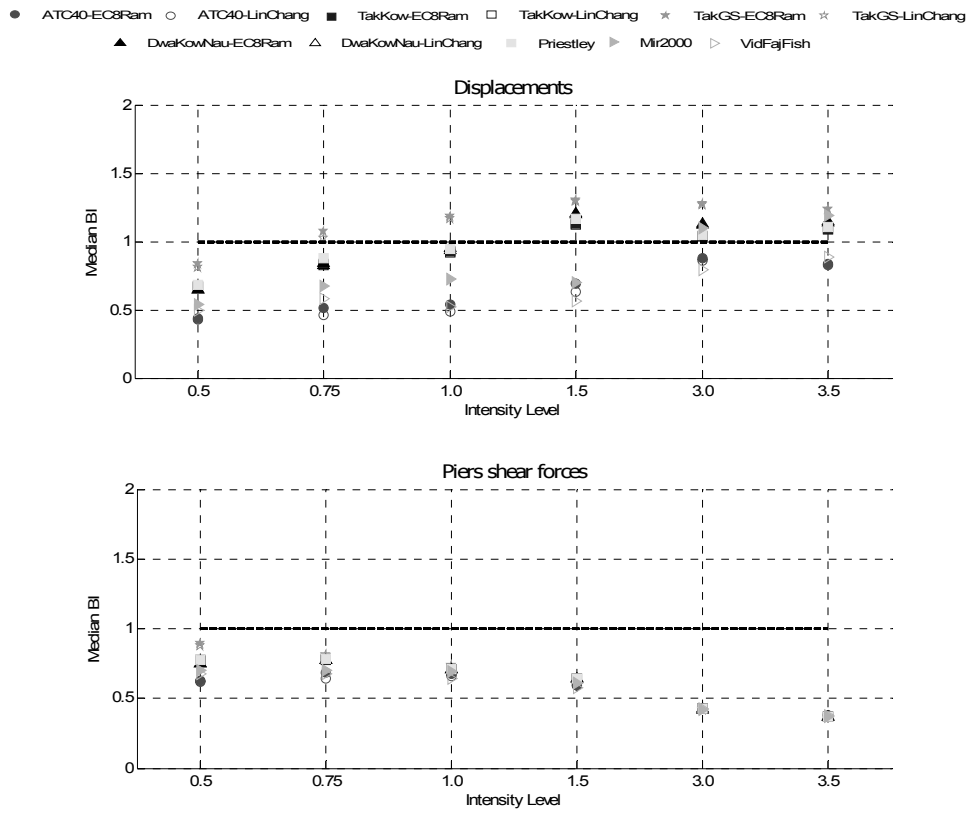

Figure 8: Median Bridge Index per intensity level.

Table 5. Median Bridge Index per intensity level - Displacements.

	Intensity Level					
Method	0.5	0.75	1.0	1.5	3.0	3.5
ATC40 - EC8Ram	0.43	0.51	0.54	0.69	0.87	0.84
ATC40 - LinChang	0.43	0.46	0.49	0.63	0.86	0.82
TakKow - EC8Ram	0.67	0.84	0.93	1.13	1.04	1.09
TakKow - LinChang	0.67	0.82	0.92	1.12	1.04	1.09
TakGS - EC8Ram	0.84	1.07	1.18	1.30	1.27	1.23
TakGS - LinChang	0.81	1.02	1.17	1.29	1.27	1.23
DwaKowNau - EC8Ram	0.65	0.85	0.95	1.21	1.13	1.14
DwaKowNau - LinChang	0.65	0.82	0.94	1.20	1.13	1.15
Priestley	0.68	0.87	0.94	1.16	1.05	1.10
Mir2000	0.54	0.67	0.72	0.70	1.10	1.19
VidFajFish	0.50	0.58	0.52	0.56	0.80	0.89

Table 6. Median Standard Deviation per intensity level - Displacements.

	Intensity Level					
Method	0.5	0.75	1.0	1.5	3.0	3.5
ATC40 - EC8Ram	0.12	0.13	0.13	0.14	0.28	0.26
ATC40 - LinChang	0.12	0.12	0.13	0.13	0.27	0.25
TakKow - EC8Ram	0.16	0.21	0.24	0.23	0.36	0.32
TakKow - LinChang	0.17	0.21	0.23	0.23	0.36	0.33
TakGS - EC8Ram	0.20	0.25	0.33	0.35	0.43	0.37
TakGS - LinChang	0.19	0.25	0.33	0.32	0.45	0.37
DwaKowNau - EC8Ram	0.15	0.19	0.22	0.27	0.40	0.35
DwaKowNau - LinChang	0.15	0.18	0.22	0.24	0.41	0.35
Priestley	0.17	0.22	0.24	0.24	0.36	0.34
Mir2000	0.15	0.15	0.18	0.15	0.29	0.28
VidFajFish	0.14	0.14	0.13	0.13	0.22	0.23

forces predictions were not significant from one bridge model to the other. Evidently, BI values are better in the case of regular bridge configurations, featuring also lower STDs. An overestimating trend for short bridges and underestimating for longer ones can also be observed, with the latter cases leading also to larger scatter. These observations stand for all response parameters considered.

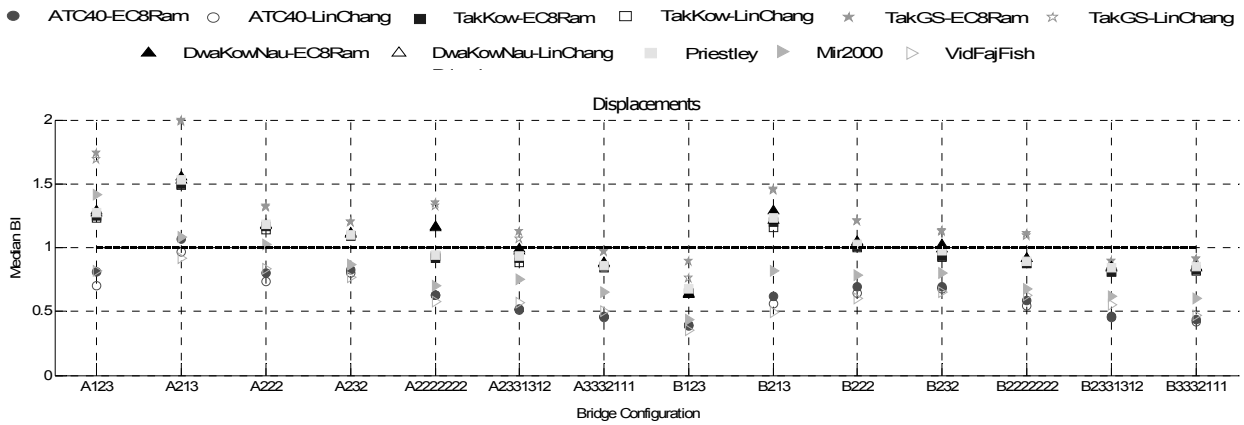

Figure 9: Median Bridge Index per bridge configuration.

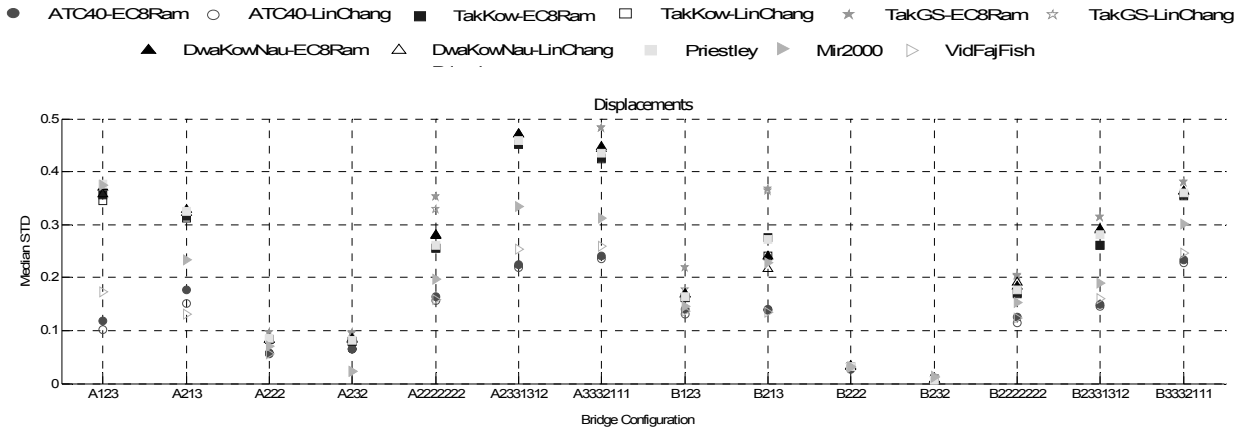

Figure 10: Median Standard Deviation per bridge configuration.

CONCLUDING REMARKS

The evaluation and comparison of eleven different possible approaches for considering the energy dissipation capacity of continuous deck bridges when assessing their performance through nonlinear static procedures (i.e. by applying spectral reduction factors), has been carried out for a large number of bridge configurations and intensity levels. Four response parameters have been chosen for comparison: deck displacements, deck bending moments, piers shear forces and abutments shear forces. Nine of the spectrum scaling schemes were damping-based whilst the other two were ductility-based. In general, results have indicated that:

- The choice of an appropriate spectral reduction method is an important issue when assessing the seismic performance of bridges, given that considerable differences have been found when employing different commonly employed approaches, especially for what concerns estimates of deck displacements.
- In particular, in case of damping-based reduction, the employed damping model proved to be much more relevant than the chosen spectral reduction equation.
- In general, damping-dependent methods perform better than their ductility-based counterparts. In particular the proposal by Priestley *et al.* [14] seemed to lead to the best predictions, very closely followed by those of Kowalsky [10] and Dwari *et al.* [13]. On the other hand, the ATC40 damping model tends to overestimate structural dissipation, leading to underestimation of displacement results.
- Typically, moments and forces were underestimated by 20-30% (with the best methods), which seems to indicate that shear amplification coefficients should perhaps be introduced in NSP formulations.
- On the other hand, with the employment of an appropriate spectral reduction factor, rather satisfactory response displacement estimates may be obtained with a nonlinear static procedure.

AKNOWLEDGEMENTS

The authors are very grateful to an anonymous reviewer, whose comments and suggestions have contributed to a significant improvement in the quality of the manuscript. Part of the current work was carried out under the financial auspices (i) of the 2005-2008 framework programme established between the Italian Department of Civil Protection and the European Centre for Training and Research in Earthquake Engineering (EUCENTRE), and (ii) of the Italian Ministry for Research and Higher Education (MiUR – Ministero dell'Università e della Ricerca) through the FIRB Project No RBIN047WCL (Assessment and Reduction of Seismic Risk to Large Infrastructural Systems). Financial support to the second author was also provided by the Portuguese Science and Technology Foundation (FCT – Fundação para a Ciência e a Tecnologia).

REFERENCES

1 Fajfar, P. (1999), "Capacity spectrum method based on inelastic demand spectra". *Earthquake Engineering and Structural Dynamics*, **28**, 979-993.

2 Chopra, A.K. and Goel, R.K. (1999), "Capacity-Demand-Diagram methods based on inelastic design spectrum". *Earthquake Spectra*, **15** (4), 637-656.

3 Miranda, E. and Ruiz-García, J. (2002), "Evaluation of approximate methods to estimate maximum inelastic displacement demands". *Earthquake Engineering and Structural Dynamics*, **31**, 539–560.

4 Miranda, E. (2000), "Inelastic displacement ratios for structures on firm sites". *ASCE Journal of Structural Engineering*, **126** (10), 1150–1159.

5 Casarotti, C. and Pinho, R. (2007), "An Adaptive Capacity Spectrum Method for assessment of bridges subjected to earthquake action". *Bulletin of Earthquake Engineering*, **5** (3), 377-390.

6 Pinho, R., Casarotti, C. and Monteiro, R. (2007), "An adaptive capacity spectrum method and other nonlinear static procedures applied to the seismic assessment of bridges". *Proceedings of the 1st US-Italy Seismic Bridge Workshop*.

7 Pinho, R., Monteiro, R. and Casarotti, C. (2009), "Assessment of Continuous Span Bridges through Nonlinear Static Procedures". *Earthquake Spectra*, in press.

8 Rosenblueth, E. and Herrera, I. (1964), "On a kind of hysteretic damping". *ASCE Journal of Engineering Mechanics*, **90** (4). 37-48.

9 Applied Technology Council (1996), Seismic Evaluation and Retrofit of Concrete Buildings. ATC-40 Report, Volumes 1 and 2. ATC, California, USA.

10 Kowalsky, M.J. (1994), "Displacement-based design – a methodology for seismic design applied to RC bridge columns". Master's Thesis, University of California at San Diego, La Jolla, California.

11 Gulkan, P. and Sozen, M. (1974), "Inelastic response of reinforced concrete structures to earthquakes motions". *ACI Journal*, 71. 604-610.

12 Iwan, W. D. (1980), "Estimating inelastic response spectra from elastic spectra". *Earthquake Engineering and Structural Dynamics*, 8. 375–388.

13 Dwairi, H.M., Kowalsky, M.J. and Nau, J.M. (2007), "Equivalent damping in support of direct displacement-based design". *Journal of Earthquake Engineering*, **11** (4), 512-530.

14 Priestley, M.J.N., Calvi, G.M. and Kowalsky, M.J. (2007), Displacement-based Seismic Design of Structures. IUSS Press, Pavia, Italy.

15 Newmark, N.M. and Hall, W.J. (1982), Earthquake Spectra and Design. Earthquake Engineering Research Institute, Berkeley.

16 Comité Europeen de Normalization (2005), Design of Structures for Earthquake Resistance, Part 2: Bridges. EN 1998-2, CEN, Brussels, Belgium.

17 Ramirez, O.M., Constantinou, M.C., Whittaker, A.S., Kircher, C.A. and Chrysostomou, C.Z. (2002), "Elastic and inelastic seismic response of buildings with damping systems". *Earthquake Spectra*, **18** (3), 531–547.

18 Lin, Y.Y. and Chang, K.C. (2003), "A study on damping reduction factors for buildings under earthquake ground motions". *ASCE Journal of Structural Engineering*, **129** (2), 206–214.

19 Vidic, T., Fajfar, P. and Fischinger, M. (1994), "Consistent inelastic design spectra: strength and displacement". *Earthquake Engineering and Structural Dynamics*, **23** (5), 507-521.

20 Casarotti, C., Pinho, R. and Calvi, G.M. (2005), Adaptive pushover based methods for seismic assessment and design of bridge structures. ROSE Research Report No. 2005/06, IUSS Press, Pavia, Italy.

21 SAC Joint Venture (1997), "Develop Suites of Time Histories". Project Task: 5.4.1, Draft Report, March 21, Sacramento, CA, USA.

22 Bommer, J.J. and Martinez-Pereira, A. (1999), "The effective duration of earthquake ground motion". *Journal of Earthquake Engineering*, **3** (2), 127-172.

23 SeismoSoft (2006), SeismoStruct – a computer program for static and dynamic nonlinear analysis of framed structures, available online from http://www.seismosoft.com.

24 Casarotti, C. and Pinho, R. (2006), "Seismic response of continuous span bridges through fibre-based finite element analysis". *Journal of Earthquake Engineering and Engineering Vibration*, **5** (1), 119-131.

25 Antoniou, S. and Pinho, R. (2004), "Development and verification of a displacement-based adaptive pushover procedure". *Journal of Earthquake Engineering*, **8** (5), 643-661.

26 Pinho, R., Casarotti, C. and Antoniou, S. (2007), "A comparison of single-run pushover analysis techniques for seismic assessment of bridges". *Earthquake Engineering and Structural Dynamics*, **36** (10), 1347-1362.

27 Bertero, V. V. (1995), "Tri-services manual methods". Vision 2000 performance based seismic engineering of buildings, Structural Engineer Association of California, Vol. 1, Part 2, Appendix J, J1–J8.

28 Bertero, V. V., Anderson, J. C., Krawinkler, H. and Miranda, E. (1991), "Design guidelines for ductility and drift limits". Rep. No. EERC/UCB 91/15, Earthquake Engrg. Res. Ctr., University of California, Berkeley

29 Reinhorn, A. M. (1997), "Inelastic analysis techniques in seismic evaluations". Seismic design methodologies for the next generation of codes, P. Fajfar and H. Krawinkler, eds., Balkema, Rotterdam, The Netherlands, 277–287.

30 Fajfar, P. (2000), "A nonlinear analysis method for performance-based seismic design". *Earthquake Spectra*, **16** (3), pp. 573–592.